Planetary and Space Science 57 (2009) 1000–1007

Contents lists available at ScienceDirect

Planetary and Space Science

journal homepage: www.elsevier.com/locate/pss

Statistical analysis of the observations of the MEX/ASPERA-3 NPI in the shadow

A. Milillo [a,*], A. Mura [a], S. Orsini [a], S. Massetti [a], P.C. son Brandt [b], T. Sotirelis [b], R. D'Amicis [a], S. Barabash [c], R.A. Frahm [d], E. Kallio [e], A. Galli [f], P. Wurz [f], M. Holmstrom [c], E.C. Roelof [b], J.D. Winningham [d], P. Cerulli-Irelli [a], S. Livi [d], R. Lundin [c], M. Maggi [a], A. Morbidini [a]

[a] INAF/Instituto di Fisica dello Spazio Interplanetario, via del Fosso del Cavaliere 100 Rome, Italy
[b] Applied Physics Laboratory, Johns Hopkins University, Laurel, USA
[c] Swedish Institute of Space Physics, Kiruna, Sweden
[d] SouthWest Research Institute, San Antonio, USA
[e] Finnish Meteorological Institute, Helsinki, Finland
[f] University of Bern, Physikalisches Institut, Bern, Switzerland

ARTICLE INFO

Article history:
Received 14 March 2008
Received in revised form
28 July 2008
Accepted 24 September 2008
Available online 15 October 2008

Keywords:
Mars
Exosphere
Energetic neutral atoms
Mars express

ABSTRACT

The analyser of space plasma and energetic atoms (ASPERA-3) neutral particle imager (NPI) on board Mars Express (MEX) is devoted to energetic neutral atom (ENA) detection within the Martian environment. These ENAs originate from the interaction between the energetic ions flowing inside the Martian environment and the exospheric neutral gas, thus providing crucial information about the dynamics of this interaction. NPI records the instantaneous angular distribution of the energy-integrated ENA signal. In order to identify recurrent ENA signals in the Martian environment, we have performed a statistical analysis of the NPI data. Count rates have been averaged using different methods in order to be able to discriminate signals coming from the planet, from a selected direction, or from specific planetographic regions at the planetary surface. Possible recurrent ENA signals (about $5 \times 10^6 (\mathrm{cm}^2\,\mathrm{sr\,s})^{-1}$) are found coming from the terminator direction and above the atmosphere toward nightside when the spacecraft was inside the planetary shadow, mainly close to the shadow edge. Some significant signal was found from the anti-Mars directions in 2005. No statistically significant signal related to pick-up ions from the atmosphere or related to magnetic anomalies above the sensor intrinsic error (estimated as $3 \times 10^6 (\mathrm{cm}^2\,\mathrm{sr\,s})^{-1}$) was observed. Our analysis shows that particular attention should be given to the use of NPI data when performing statistical studies; in fact, the sensor has some intrinsic limitations due to inadequate UV suppression, difficulties in sector inter-calibrations, and variations in the sector response versus time.

1. Introduction

The plasma and neutral particle package, analyser of space plasma and energetic atoms (ASPERA-3) (Barabash et al., 2004), has been operating on board ESA Mars Express (MEX) spacecraft since orbit insertion in December 2003. The ASPERA-3 instrument that includes four sensors: an electron spectrometer (ELS), an ion analyser (IMA), and two different energetic neutral atom (ENA) sensors: the neutral particle imager (NPI, an ENA imager with high angular resolution, but with no mass and energy resolution) and the neutral particle detector (NPD, a neutral mass analyser that can resolve both particle velocities and masses, with lower angular resolution). NPI is devoted to ENA imaging of the signal generated in the Martian environment by the interaction between the solar wind (SW) and the upper atmosphere.

Since the SW interacts with Mars mainly through the ambient atmospheric/exospheric gas (Kallio et al., 1997, 2006), charge-exchange is expected to be very effective. Several numerical simulations have been performed to study such interaction, including different ion/neutral sources: supersonic and shocked SW (Holmström et al., 2002), and accelerated planetary ions (Barabash et al., 2002; Lichtenegger et al., 2002). Charge-exchange ENAs may also emerge from the SW interaction with the atmosphere of Phobos (Mura et al., 2002). Other processes, like atmospheric atoms sputtered by picked-up O^+ ions (Johnson and Luhmann, 1998) and SW protons backscattered from the Martian exosphere (Kallio and Barabash, 2001; Holmström et al., 2002), can be responsible for additional neutral emission. Hence, ENA

* Corresponding author.
E-mail address: anna.milillo@ifsi-roma.inaf.it (A. Milillo).

0032-0633/$ - see front matter © 2008 Elsevier Ltd. All rights reserved.
doi:10.1016/j.pss.2008.09.016

imaging is a potentially useful tool to understand the geometry, the physics, and the dynamics of the plasma and the escape mechanisms around Mars.

ENA signals have been detected and fruitfully analysed in dedicated studies of specific events by the ASPERA-3/NPD sensor (e.g., Futaana et al., 2006; Galli et al., 2006) and by the NPI sensor on the nightside (Brinkfeldt et al., 2006; Gunell et al., 2006). Mura et al. (2007) and Galli et al. (2008) successfully performed a statistical analysis of the NPD ENA data from the dayside and nightside, respectively.

In order to identify recurrent ENA signals in the Martian environment, we have performed a statistical analysis of the available NPI data covering two time periods: from January 25th 2004 up to September 15th 2005 and from September 24th up to December 14th. We have averaged the data using several methods in order to be able to discriminate between those signals which come from the planet, and those which come from selected directions depending on relative Sun positions or those which come from specific locations close to the surface, possibly linked to planetary features like magnetic anomalies.

In this paper, we will present a brief description of the NPI characteristics and the MEX position during the eclipse seasons in Section 2 followed by a description of the possible nightside ENA sources that the present analysis intends to discuss in Section 3. In Section 4, the statistical analysis procedure used to analyse the NPI data is described. From this process, maps of the average signal as emitted from the planet are created and are described in Section 5. In Section 6, the maps for each spacecraft position during eclipse seasons, obtained by averaging the signal for specific look directions, are discussed. The maps of the emitted signal coming from specific planetary regions have been obtained by considering the planetographic coordinates and comparing them to magnetic anomaly maps (Section 7). The summary and conclusions of this work are given in Section 8.

2. Neutral particle imager

NPI (Fig. 1) measures the integral ENA flux (in the energy range 0.1–60 keV) without mass and energy resolution, but with good angular resolution, $4.5^\circ \times 11.25^\circ$ (Barabash et al., 2004). The incoming ENAs are reflected by a coated target block before being detected by a 32 sector anode, covering a total $360^\circ \times 5^\circ$ field-of-view (FOV). In its MEX configuration, NPI sectors 15 and 16 are physically blocked by the spacecraft. The time resolution of the data collected in a telemetry packet is 1 s. The geometrical factor of each sector is $G = 2.7 \times 10^{-3}\,\mathrm{cm^2\,sr}$, while the efficiency of the instrument is energy dependent (e.g., for 1 keV neutrals $\varepsilon = 4 \times 10^{-4}$) (Holmstrom et al., 2006; Brinkfeldt, 2005). Hence, a count rate of $1\,\mathrm{s^{-1}}$ would correspond to a 1 keV flux of $f = 1/G, \varepsilon = 9 \times 10^5\,(\mathrm{cm^2\,sr\,s})^{-1}$.

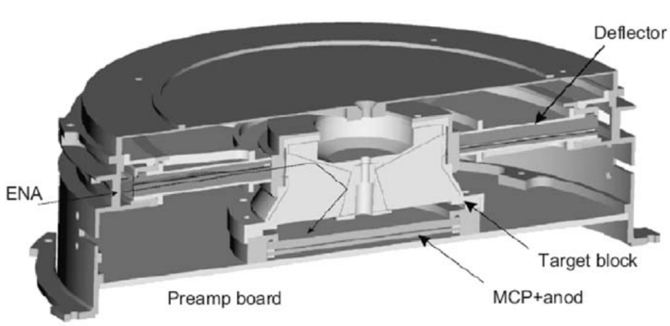

Fig. 1. NPI geometry.

The NPI detector is known to be strongly affected by UV contamination; hence, a careful data analysis is needed. Furthermore, Holmstrom et al. (2006) have shown that different sectors have different responses to ENAs, with varying sensitivity, β, and background noise levels, α. Moreover, the α values show time variations. In order to avoid the UV contamination, we have selected only those data collected during periods of spacecraft eclipse. This is known as deep-shadow condition (sdw). Solar eclipse positions were selected since outside of this region, sectors in the anti-sun direction are found to be affected by electronic cross-talk caused by Solar UV (Holmstrom et al., 2006). Furthermore, atmospheric UV emission is observed outside of eclipse and it must be avoided as well.

Figs. 2a and b show the spacecraft position during the eclipse seasons of 2004 and 2005, respectively. The spacecraft is mostly in the Southern hemisphere during 2004; whereas, it is mainly in the Northern hemisphere during 2005. Note that NPI was not always operative during the eclipse periods.

3. ENA sources in the shadow of Mars

A likely source of ENAs results from charge-exchange of the SW with the atmosphere. However, since we impose the sdw, we are investigating ENAs produced by deflected SW which has a velocity component perpendicular to the shadow cylinder of the planet. In fact, theoretical models (e.g., Kallio et al., 2006) foresee that the shocked SW inside the Mars magnetosheath produces ENAs directed tailward that, thanks to non-zero temperature, have a component toward the planet shadow. A proof of this ENA signal was recently obtained by Galli et al. (2008) from the 23 April to 26 May 2004 statistical analysis of NPD data, when the spacecraft was in the nightside of Mars and inside the induced magnetosphere boundary. The ENA signal between 0.2 and 10 keV has maximum intensity ($2.4 \times 10^5\,\mathrm{cm^{-2}\,s^{-1}\,sr^{-1}}$) for look directions, which are closest to the planet terminator (i.e., the limb close to the Sun direction). The observed ENA signal comes from a broader region (look directions extending more than 60° from the limb) than that expected by theoretical models. Hence, ENAs seem to be generated mainly close to the planetary terminator, but also in a broad region above the planet. Galli et al. (2008) suggested that the contribution of planetary ions should be responsible for such a discrepancy. In this case, pick-up ions can also be a source for ENAs. The generated ENAs should again come from close to the terminator toward the nightside, but in this case they should be preferentially lost in the direction of the electric field (Fedorov et al., 2006). An IMF clock angle asymmetry in ENA signal would be a proof that such a generation mechanisms is active.

Backscattered ENAs in the dayside have been reported by Futaana et al. (2006). The same process could, in principle, occur when ions precipitate toward the nighside atmosphere from the tail. Galli et al. (2008) estimated an upper limit of about $10^4\,\mathrm{cm^{-2}\,s^{-1}\,sr^{-1}}$ for this ENA signal.

Finally, another possible ENA generation region could be related to magnetic anomalies (Purucker et al., 2000). Magnetic anomalies trap electrons (Mitchell et al., 2007) and can, in principle, trap ions as well. In fact, if this is the case, trapped ions can charge-exchange with atmospheric neutrals thus generating radiating ENAs. This process can also occur on the planet's nightside toward the dusk terminator. The ENA signal should decrease on the nightside of Mars toward dawn as the electrons and ions trapped in the minimagnetospheres recombine during the planet rotation.

4. Data analysis

In our analysis we have used the count corrections computed for the years 2004 and 2005, as estimated in Holmstrom et al. (2006).